Received: 11 January 2019 | Revised: 1 May 2019 | Accepted: 17 May 2019

DOI: 10.1002/jbm.b.34425

ORIGINAL RESEARCH REPORT

# Characterization of ageing resistant transparent nanocrystalline yttria-stabilized zirconia implants

Nami Davoodzadeh[1] | Mildred S. Cano-Velázquez[2] | David L. Halaney[1] | Ariana Sabzeghabae[1] | Gottlieb Uahengo[3] | Javier E. Garay[3] | Guillermo Aguilar[1]

[1]Department of Mechanical Engineering, University of California – Riverside, Riverside, California

[2]Instituto de Investigaciones en Materiales, Universidad Nacional Autónoma de México, México, Mexico

[3]Department of Mechanical and Aerospace Engineering, University of California – San Diego, La Jolla, California

**Correspondence**
Guillermo Aguilar, Department of Mechanical Engineering, University of California – Riverside, Riverside, California.
Email: gaguilar@engr.ucr.edu

**Funding information**
Consejo Nacional de Ciencia y Tecnología, Grant/Award Number: 741249; Division of Materials Research, Grant/Award Number: 1547014; Office of International Science and Engineering, Grant/Award Number: 1545852; National Science Foundation (NSF)

## Abstract

The "Window to the Brain" is a transparent cranial implant under development, based on nanocrystalline yttria-stabilized zirconia (nc-YSZ) transparent ceramic material. Previous work has demonstrated the feasibility of this material to facilitate brain imaging over time, but the long-term stability of the material over decades in the body is unknown. In this study, the low-temperature degradation (LTD) of nc-YSZ of 3, 6, and 8 mol % yttria is compared before and after accelerated ageing treatments following ISO standards for assessing the ageing resistance of zirconia ceramics. After 100 hr of accelerated ageing (equivalent to many decades of ageing in the body), the samples do not show any signs of phase transformation to monoclinic by X-ray diffraction and micro-Raman spectroscopy. Moreover, the mechanical hardness of the samples did not decrease, and changes in optical transmittance from 500 to 1000 nm due to ageing treatments was minimal (below 3% for all samples), and unlikely to be due to phase transformation of surface crystals to monoclinic. These results indicate the nc-YSZ has excellent ageing resistance and can withstand long-term implantation conditions without exhibiting LTD.

**KEYWORDS**
ageing resistance, implant, low-temperature degradation, transparent nanocrystalline yttria-stabilized zirconia, zirconia ceramic

## 1 | INTRODUCTION

Polycrystalline zirconia-based ceramics have become the focus of recent investigations because of their unique combination of properties. Their high hardness and chemical inertness (high temperature stability and corrosion resistance) make them important target materials for various applications. Well-proven biocompatibility, low thermal conductivity, and high oxygen diffusivity (Nakamura, Kanno, Milleding, & Ortengren, 2010) have made zirconia-based ceramics a favorable option for biomedical applications. By decreasing the grain size of the polycrystalline ceramics to nanoscale, novel characteristics such as high density (low porosity), transparency/translucency, and high refractive index and Abbe number have been reported (Anselmi-Tamburini, Woolman, & Munir, 2007; Casolco, Xu, & Garay, 2008; Grasso, Kim, Hu, Maizza, & Sakka, 2010; Rosenflanz et al., 2004; Xiong, Fu, Pouchly, Maca, & Shen, 2014).

Recently, we have investigated the application of transparent nanocrystalline yttria-stabilized zirconia (nc-YSZ) ceramics as a biomedical transparent cranial implant, referred to in the literature as "Window to the Brain" (WttB) implant. The concept is illustrated in Figure 1. These transparent implants aim to provide chronic optical access to the brain (Aminfar, Davoodzadeh, Aguilar, & Princevac, 2019; Cano-Velázquez et al., 2018; Davoodzadeh et al., 2019; Davoodzadeh, Cano-Velázquez, et al., 2018; Davoodzadeh, Cuando, Aminfar, Cano, & Aguilar, 2018; Halaney et al., 2018) to facilitate the diagnosis and treatment of neurological diseases (Damestani et al., 2013). A recent study also demonstrated the ability of this implant to

  

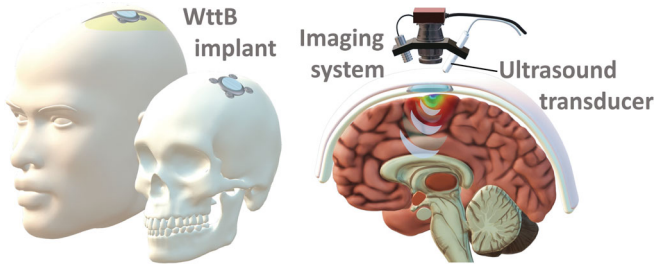


**FIGURE 1** Illustration of the Window to the Brain cranial implant concept. The implant will be attached to the skull beneath the scalp, to allow for optical and ultrasonic transmission to and from the brain

improve ultrasound imaging of the brain compared to imaging through skull (Gutierrez et al., 2017). The transparency of the nc-YSZ is achieved by using ultra-fine yttria-stabilized zirconia (YSZ) powder and an innovative ceramic processing method, current-activated pressure-assisted densification (CAPAD), leading to transparent nc-YSZ ceramics (Alaniz, Perez-Gutierrez, Aguilar, & Garay, 2009). CAPAD enables reduction of the number of pores as well as reduction of their dimensions to nanometric scale and at these length scales, porosity is sufficiently small to minimize scattering in the spectral range of interest for medical imaging and laser therapies of the brain (Casolco et al., 2008).

Although zirconia-based implants have been known for their excellent mechanical properties, the in vivo application was found to be affected by long-term failures for some samples with micrometric grain sizes, due to low temperature degradation (LTD). By contrast, YSZ with nanometric size grains are significantly more resistant to LTD (Anselmi-Tamburini et al., 2007). LTD is due to a crystal phase transformation from tetragonal to monoclinic, which is associated with a volume increase of about 4–6% (Chevalier, Cales, & Drouin, 1999). This expansion induces localized compressive stresses and eventually microcracks around the transformed zirconia particles (Lughi & Sergo, 2010). These microcracks propagate through the sample bulk, and internal defects such as pores and crack surfaces (Chevalier, Gremillard, & Deville, 2007). Under such conditions, the material loses its cohesion and mechanical properties. Therefore, small amounts of porosity contribute to enhance the nucleation and propagation of the monoclinic phase, so the use of very dense implants is required to reduce the transformation rate (Lughi & Sergo, 2010; Muñoz-Saldaña & Balmori-Ramírez, 2003).

As a modest amount of transformation can change optical characteristics such as transparency, in this study we investigated the optical properties of transparent nc-YSZ ceramics with different stabilizer contents (yttria dopant levels) of 3, 6, and 8 mol % before and after extended accelerated ageing treatments. Further, because mechanical properties become compromised when LTD occurs, we also compared the hardness of our samples before and after the accelerated ageing treatments. The treatment simulates in vivo ageing, according to the ISO 13356:2008 recommendations (Chevalier et al., 2007; Deville, Chevalier, & Gremillard, 2006) (i.e., autoclave processing at 134°C at a water partial pressure of 2–3 bar).

To our knowledge, this is the first study to compare the LTD of transparent nanocrystalline YSZ with differing stabilizer content (3, 6, and 8 mol % yttria). Most studies conducted on LTD of zirconia-ceramic have involved opaque micrometric-grained YSZ. The objective of this current study is to assess the LTD of nc-YSZ through simulated ageing protocols, to model how the WttB implant will perform optically and mechanically over decades of ageing in the body.

## 2 | EXPERIMENTAL SECTION

### 2.1 | Implant fabrication and preparation

Commercial (Tosoh USA Inc., Grove City, OH) nanocrystalline 3YSZ, 6YSZ, and 8YSZ powders (respectively doped with 6, 12, and 16 mol $\%YO_{1.5}$ nc-YSZ) with reported crystallite sizes of 55 nm, were densified via the current activated pressure assisted (CAPAD) technique, to produce transparent yttria-stabilized zirconia ceramics (Garay, 2010). In the literature, this technique is often called spark plasma sintering (SPS). We used CAPAD here to emphasize the fact that it is complimentary contributions of the current and an applied pressure that makes it successful (Garay, 2010). During the fabrication processes of all samples for this work, 1.5000 g ± 0.0001 g of starting powder was poured into a graphite die of inner diameter measuring 19 mm, and secured between two plungers with the same outer diameter. The die, plungers, and powder assemblies were placed into the CAPAD apparatus and secured between two graphite spacers and copper electrodes, all enclosed within a vacuum chamber. A vacuum of $1 \times 10^{-3}$ Torr was attained in all cases.

All powder compacts were prepressed to a maximum load of 30 kN, applied linearly, to produce a nominal compressive pressure of 106 MPa on the sample, and held for 2 min to achieve a green body of appreciable density. The load was then released, and the green body subjected to another uniaxial compressive stress of 106 MPa over a 3-min interval. Once the set-point temperature was reached, a second load ramp ( kN $min^{-1}$) was applied. This ramp bringing the uniaxial pressuring on the sample up to 141 MPa, was maintained for 10 min, the duration of processing, and thereafter linearly released. In addition to the aforementioned load parameters, the green pellet was simultaneously heated to high temperature by applying electric current through the die and plunger assembly, consequently creating joule heating. All samples were processed at 1200°C, with an average heating rate of approximately 160°C/min, from room temperature, and held for 10 min.

The density of the samples was measured using the Archimedes method, and the ASTM standard designated B962-13 was followed (ASTM B962-13, 2009). Grain size measurements of the bulk sample made from fracture surfaces were evaluated using SEM.

The samples thicknesses were reduced by polishing with 30-micron diamond slurry on an automatic polisher (Pace Technologies, Tucson, AZ). The two faces were then polished using progressively finer abrasives (from 30 μm diamond slurry down to 0.2 μm

colloidal silica slurry) to reduce light scattering by the implant surfaces and thus increase transparency as well as to create a uniform surface area between different samples. As ageing begins at surface and propagates into bulk, surface area is an important factor to control between samples when comparing ageing results. After preparation process, the polished samples underwent ageing tests.

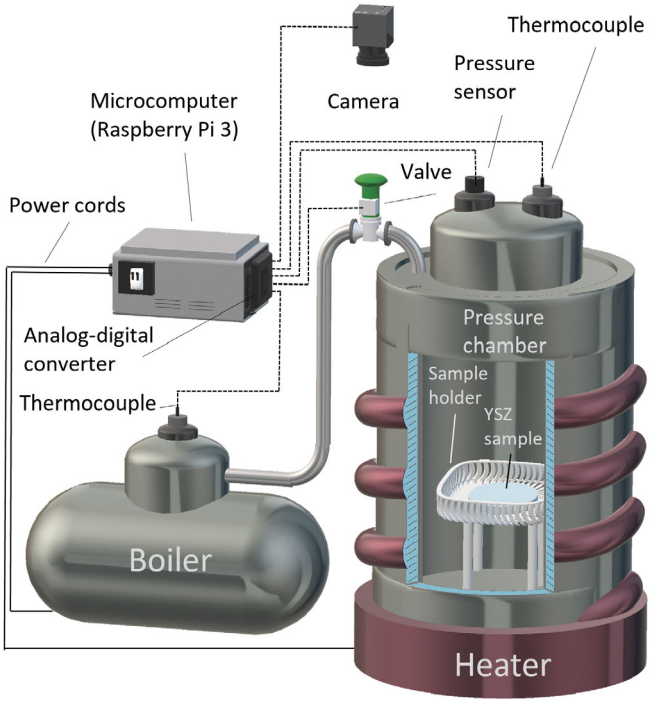


**FIGURE 2** Hydrothermal treatment experimental setup schematic. Samples were placed inside a pressure chamber. Thermocouples and a pressure sensor coupled to a microcomputer maintained the temperature and pressure at 134°C and 2–3 bar

## 2.2 | Ageing test

The test for simulating in vivo ageing, per the ISO 13356:2008 recommendations (ISO, 2008), uses hydrothermal treatment at 134°C, at a steam partial pressure of 2–3 bar which is known as autoclave processing. As seen in Figure 2, the samples were placed in a steel pressure chamber, and saturated high-pressure steam was generated by a boiler and sent to the sample chamber through an electronic valve. An electric heating jacket surrounded the chamber to prevent steam condensation and stabilize the temperature at 134°C. Two K-type thermocouples were used to measure the sample chamber and the boiler temperature, and an electronic pressure sensor was connected to the pressure chamber. A microcomputer (Raspberry Pie 3) coupled to the sensors controlled the heating jacket power and the valve status. The ageing treatments were performed in cycles of 5, 10, 10, 25, 25, 25 hr, for a total of 100 hr for each sample. At the end of the treatments, the samples were cooled down to room temperature and dried.

## 2.3 | Material characterization

X-ray diffraction (XRD) analysis was used to detect any phase transformation due to the ageing treatments (Figure 3a). Due to its simplicity, this technique has been considered as a first step to investigate the ageing sensitivity of a particular zirconia. However, this technique suffers some limitations, such as poor precision during the first stages of ageing (which have also been reported with a much higher sensitivity using grazing incidence angles of 1–5° ($2\theta$)) (Chevalier et al., 2007; Keefer & Michalske, 1987) as well as the absence of local information on ageing processes (Chevalier, 2006). Data were acquired on an X-ray diffractometer (PANalytical Empyrean Series 2) using a step size of 0.03° ($2\theta$) and an acquisition time of 5 s per step. Various (hkl) planes were used to evaluate crystal structures, including cubic (111),

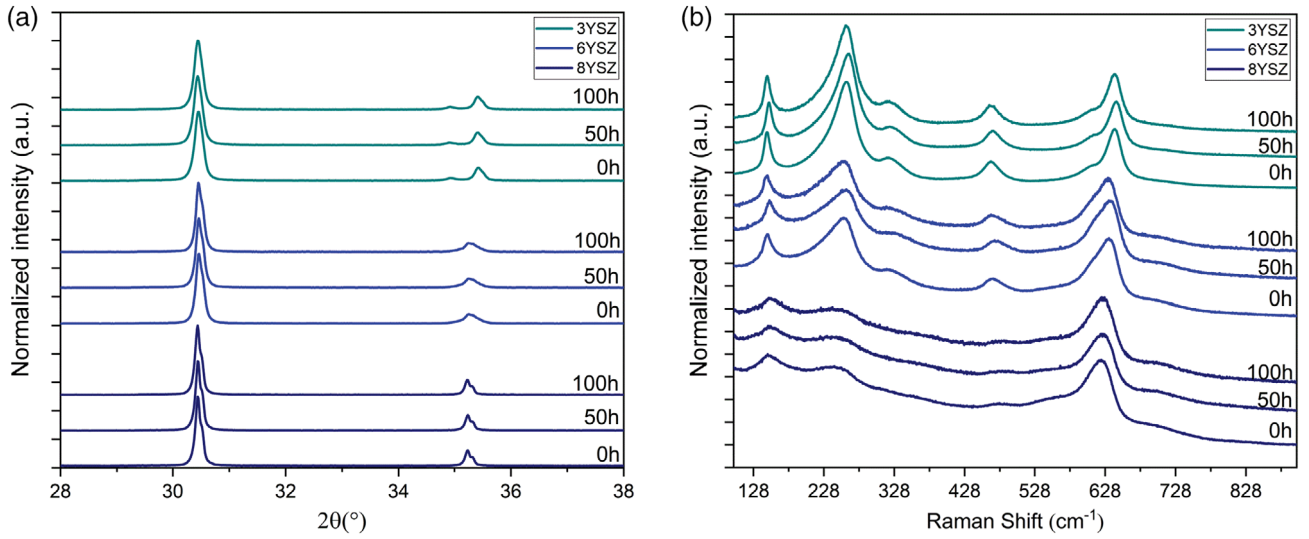


**FIGURE 3** For 3YSZ, 6YSZ, and 8YSZ, XRD diffractogram (a) and micro-Raman patterns (b) obtained after up to 100 hr of hydrothermal treatment at 134°C. XRD, X-ray diffraction; YSZ, yttria-stabilized zirconia

tetragonal (101), and monoclinic ($\bar{1}11$ $\bar{1}11$ and 111) peaks at 30.2°, 30.2°, 28.2°, and 31.5° ($2\theta$), respectively. It must be noted that the distance between cubic and tetragonal peaks is smaller than the width of the peaks which makes them indistinguishable and detected at the same angle (30.2°).

Raman spectroscopy was additionally performed to investigate the impact of ageing on the phase transformation (Figure 3b). Raman spectroscopy has been reported to show higher sensitivity to the smaller trace of monoclinic phase (Kim, Jang, & Lee, 1997), associated with a higher lateral resolution than XRD (Grasso et al., 2010). Micro-Raman spectrum were recorded by using a spectrometer (Horiba's LabRam) with acquisition time of 60 s. The incident laser light with a wavelength of 532 nm was focused on the sample within a spot of 10 μm in diameter. Presence of monoclinic phase was assessed by comparing monoclinic doublet at 179 and 190 $cm^{-1}$ in the Raman spectra.


**FIGURE 4** Photographs of an NBS 1963A resolution target (a) through the 3YSZ (b), 6YSZ (c), and 8YSZ (d) samples. The resolutions shown are the 18 cycle/mm target (each black line width is 27.78 μm). NBS, National Bureau of Standards; YSZ, yttria-stabilized zirconia

## 2.4 | Optical characterization

To qualitatively compare the transparency of the densified and polished 3YSZ, 6YSZ, and 8YSZ samples, photographs of a NBS 1963A resolution target (18 cycle/mm target, each black line width is 27.78 μm) through the ceramics were taken (Figure 4). For quantitative comparison, optical transmittance of the nc-YSZ samples were evaluated by optical spectrometry in visible and near-infrared light. The optical transmittance was measured using a white light source (HL2000 FHSA, Ocean Optics, FL) and a spectrometer (SD2000, Ocean Optics, FL) in the 500–1000 nm wavelength range. The sampling system used for specular transmittance consists of a rail coupled with two fiber holders including collimating lenses (MP-74-UV, Ocean Optics, FL) with a wavelength range of 185–2500 nm. A space for placing the samples was incorporated on one of the fiber holders. After placing the sample, the fiber holders were fixed by screws to mitigate the effects of ambient light. A couple of multimodal optical fibers (P400-2-VIS-NIR, Ocean Optics, FL) were connected from the light source to the fiber holder and from the other fiber holder to the spectrometer. The spectra were acquired as an average of 10 measurements, with integration time of 100 ms.

The normalized transmittance was calculated considering the ratio of light transmitted through the sample to the total light incident upon that sample [Equation (1)].

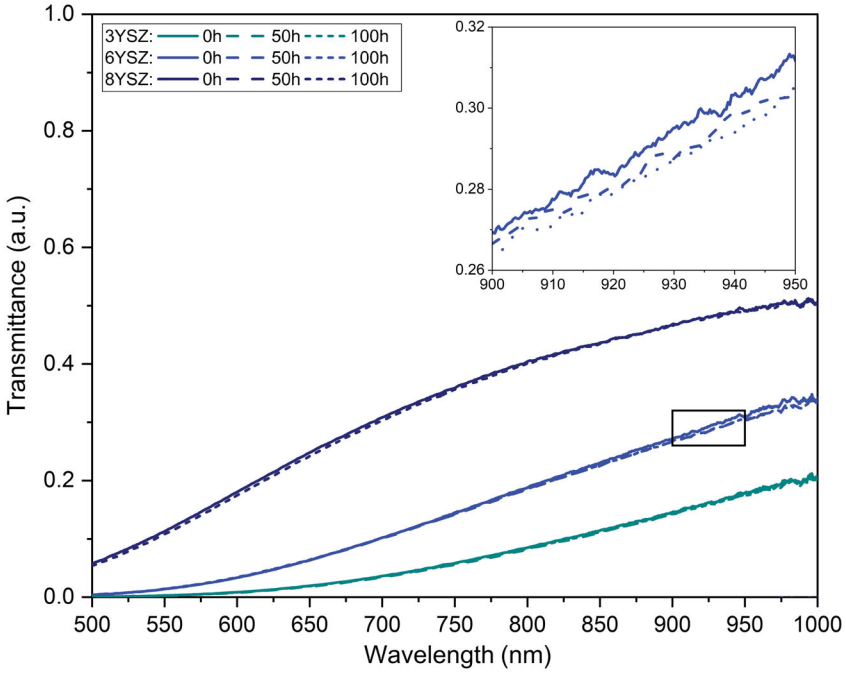


**FIGURE 5** Mean $T(\lambda)$ values obtained at wavelength range of 500–1000 nm to compare the transmittance values of various nc-YSZ samples (3YSZ, 6YSZ, and 8YSZ) before and after ageing. The inset shows the maximum difference in optical properties curves between the pristine and aged samples. YSZ, yttria-stabilized zirconia

$$T(\lambda) = \frac{S(\lambda) - D}{I(\lambda) - D} \quad (1)$$

where $T$ is transmittance, $S(\lambda)$ is the measured spectral intensity, $I(\lambda)$ is the total light incident, and $D$ represents the reference in dark environment.

### 2.5 | Mechanical characterization

To compare the mechanical properties between the pristine samples and aged samples, indentation tests were performed using a micro Vickers hardness tester (900-391A, Phase II Plus, NJ). The indentation was performed using loading force of 4.9 N and 15 s duration. The instrument was recalibrated before and after testing, by performing a series of indentations on a certified steel reference sample. The average value and *SD* of 10 indentations were calculated for each sample before and after the ageing treatments.

## 3 | RESULTS

### 3.1 | Densified samples

The density of the CAPAD processed samples (discs of 1 mm thickness and 19 mm diameter) were 99.8%, 99.9%, and 99.9% for the 3YSZ, 6YSZ, and 8YSZ, respectively. Grain size measurements of the bulk samples were made from fracture surface measurements of SEM micrographs and showed an average grain size (AGS) of 147 ± 45 nm across all compositions. The polished sample thicknesses were 610 ± 1 μm, 584 ± 1 μm, and 601 ± 1 μm for 3YSZ, 6YSZ, and 8YSZ, respectively.

### 3.2 | Material characterization

Phase transformation to monoclinic was assessed with XRD and micro-Raman Spectroscopy. XRD patterns of samples before and after 50 and 100 hr of accelerated ageing via hydrothermal treatment are shown in Figure 3a. XRD patterns in the range of 28°–38° are shown in Figure 2a. Only cubic (111) and tetragonal (101) (both peaks inseparably appeared at 30.2°) can be seen in the XRD patterns, confirming that there is no monoclinic phase present. The peaks and patterns remained the same for all samples following ageing treatments, indicating that no phase transformation occurred. In Figure 3b, the comparison of micro-Raman patterns in the 100–900 $cm^{-1}$ region shows stability of tetragonal and cubic phases after the treatments, further confirming that no phase transformation to monoclinic (doublet at 179 and 190 $cm^{-1}$) occurred.

### 3.3 | Optical characterization

Figure 4 shows images of a National Bureau of Standards resolution target imaged through the transparent nc-YSZ samples. All of the samples clearly show the highest resolution (18 cycles/mm) on the resolution target when transmitted light is observed through them. As seen in Figure 3, all the samples transmit light and appear as different shades of orange.

To assess any change in optical properties due to the accelerated ageing hydrothermal treatment, optical transmittance of the transparent samples was measured over the wavelength range of 500–1000 nm at baseline and after 50 and 100 hr of ageing. Figure 5 presents the normalized optical transmittance, $T(\lambda)$, for both pristine and aged 3YSZ, 6YSZ, and 8YSZ samples. As shown in the figure, the transmittance curves for all three samples have approximately the same trend. However, for any given wavelength, the transmittance increases as the yttria content is increased. In addition, the samples transmit a higher percentage of light as the wavelength of the incident light is increased. These results are consistent with our previous measurements, showing relatively low transmission in the blue-green end of spectrum caused by absorption of oxygen vacancy related defects (Alaniz et al., 2009). The insets in Figure 4 show the maximum difference between the transmittance curves between pristine and aged samples. The changes in transmittance values after the treatments (compared to the pristine samples), were less than 3%.

**TABLE 1** Hardness of the pristine and aged samples

| | Hardness (GPa) | | |
|---|---|---|---|
| Sample | Pristine | After 50 hr | After 100 hr |
| 3YSZ | 13.84 ± 0.20 | 13.80 ± 0.16 | 13.71 ± 0.21 |
| 6YSZ | 12.92 ± 0.10 | 13.16 ± 0.11 | 13.13 ± 0.13 |
| 8YSZ | 13.22 ± 0.12 | 13.16 ± 0.18 | 13.17 ± 0.13 |

*Note:* Data is given with *SD* (statistical processing of multiple indentations for each sample).
Abbreviation: YSZ, yttria-stabilized zirconia.

### 3.4 | Hardness characterization

As the phase transformation to monoclinic compromises mechanical properties, we compared the hardness of 3YSZ, 6YSZ, and 8YSZ before and after ageing. The averaged results and the standard deviations calculated from 10 indentation experiments per sample are summarized in Table 1 as a function of ageing treatment time and yttria content. For the pristine samples, the highest hardness value was obtained for 3YSZ sample. The 6YSZ and 8YSZ samples had slightly lower hardness values (6.64% and 4.26%, respectively). For 3YSZ and 8YSZ samples, changes in hardness were not significant (paired two-tail $t$ test), with $t$ values greater than 0.05. For the case of 6YSZ, changes in hardness between pristine sample and sample after 50 or 100 hr of ageing treatment was found to be significant ($t$ = 0.00094 and 0.0037, respectively), although these changes were small (less than 2% increase in hardness compared to pristine sample).

## 4 | DISCUSSION

The transparent nc-YSZ ceramics evaluated in this study show promise for medical and nonmedical applications. Previously, we have

investigated the application of 8YSZ for creating transparent cranial implants. By performing biocompatibility tests and brain imaging studies, we have demonstrated the feasibility of this application (Aguilar, Davoodzadeh, Halaney, Uahengo, & Garay, 2018; Aminfar et al., 2019; Cano-Velázquez et al., 2018; Damestani et al., 2013; Damestani, Galan-Hoffman, Ortiz, Cabrales, & Aguilar, 2016; Davoodzadeh, 2017; Davoodzadeh et al., 2019; Davoodzadeh, Cano-Velázquez, et al., 2018; Davoodzadeh, Cuando, et al., 2018; Gutierrez et al., 2017; Halaney et al., 2018). Phase transformation (ageing) resistance and the effect of hydrothermal treatment on optical and mechanical properties of the ceramics are crucial to understand for any medical or nonmedical application of the transparent nc-YSZ ceramics. Recently, fabrication of translucent and transparent YSZ with grain size on the microscale and nanoscale have been reported (Aguilar et al., 2018; Casolco et al., 2008; Xiong, Fu, Pouchly, Maca, & Shen, 2014; Zhang et al., 2015). However, a thorough investigation on preparation and evaluation of LTD and its influence on mechanical and optical properties in transparent nanocrystalline stabilized zirconia ceramics with various yttria dopant levels of 3, 6, and 8 mol % have not been reported.

Ageing caused by the transition of the tetragonal-to-monoclinic phase represents a common problem of zirconia ceramics stabilized by acceptor dopants. The process is triggered by the hydroxyl groups (with bound –OH) which can penetrate into the lattice over time through oxygen vacancies resulting from the doping process (Alaniz et al., 2009). Degradation due to this transformation has been known to propagate gradually to the bulk of the material (Chevalier et al., 1999). Unlike the porosity of micrometric-structured stabilized zirconia ceramics, the nanoscale grain and high densities of our nc-YSZ have proven highly effective in preventing the transformation, as shown by our results here as well as others (Tredici et al., 2016; Wei & Gremillard, 2018).

Considering the self-ionization of water, a greater number of $OH^-$ ions produced at higher temperatures and pressures can accelerate the LTD process (Pitzer, 1982). Accelerated ageing treatment has been a common method to evaluate zirconia ceramic LTD. Chevalier and Gremillard's evaluation based on actual observations of zirconia femoral heads implanted in vivo for 4 and 8 years, showed that 1 hr of autoclave treatment at 134°C had a similar effect as a 3–4 years in vivo ageing (Chevalier et al., 2007). They proved that the ISO standard recommendations for determining the long-term duration of prosthetic zirconia were inadequate (Perrichon et al., 2017) and the ISO recommendation was revised according to Gremillard's suggestions (ISO 13356:2008, 2008). Advances in grain size reduction resulted in YSZ ceramics that are more resistant against LTD, and for this reason Sanon et al. recommended to increase the ageing test up to 100 hr for better observation of the LTD process. Our simulation was extended to 100 hr following Sanon's proposal (Sanon, Chevalier, Douillard, & Cattani-Lorente, 2015). Given the very high LTD resistance that nanostructured YSZ ceramics have shown compared to conventional microcrystalline YSZ ceramics, a new accelerated ageing simulation protocol will be needed to characterize any transformation and degradation which may occur in these samples (Sanon et al., 2015).

We have shown our 3YSZ, 6YSZ, and 8YSZ samples with AGS of 147 nm ± 45 nm, prepared using CAPAD, satisfy the requirements for long-term performance as an optical implant. Indeed, for all the investigated samples the increase in monoclinic phase content was below the XRD and micro-Raman detection range, in agreement with our previous findings (Aguilar et al., 2018). The ageing tests showed the ability of these materials to withstand common sterilization treatments as well. LTD resistant YSZ samples have been reported recently, however they are produced using the conventional zirconia doped 3 at% of yttria (Lucas, Lawson, Janowski, & Burgess, 2015; Wei & Gremillard, 2018), often codoped with other cations (Zhang et al., 2016). In these studies, the samples were sintered by pressureless techniques with resulting grain sizes of hundreds of nanometers (Lucas et al., 2015; Zhang et al., 2015, 2016). YSZ samples prepared by CAPAD (or SPS) with nanometric grain size have also been shown by others to have very high LTD resistance and density (Tredici et al., 2016; Xiong et al., 2014). It should also be noted that YSZ samples with similar grain size, mechanical properties, and aging resistance have been produced using more conventional multistep sintering methods (Wei & Gremillard, 2018).

Optical characterization of the pristine samples shows the optical transmittance is highly dependent on the yttria dopant level. Higher transmittance was found for the sample Fs with higher yttria dopant content, although the spectral behaviors are similar for the three sample types (3YSZ, 6YSZ, and 8YSZ). This indicates the increase in the yttria content which resulted in higher cubic content favors increased transparency (Casolco et al., 2008). Decreased symmetry of the tetragonal structure causes asymmetric scattering in the 3YSZ sample while the more isotropic structure in the 6YSZ and 8YSZ reduces light scattering (Casolco et al., 2008; Kodera, Hardin, & Garay, 2013). This difference in crystal structure is the likely cause of the differences in light transmittance. 8YSZ is the most transparent sample, allowing the transmittance of light in a wider wavelength range, starting on 610 nm. The 3YSZ sample is the least transparent. In addition, we have shown the optical property values have a maximum change of 3% after 100 hr of the hydrothermal treatments in wavelength range of 500–1000 nm for all the samples. This small change is unlikely to be caused by surface crystal phase changes, and may instead be due to measurement error.

The hardness of our nanometric YSZ samples, both pristine and aged, compare well with similar YSZ materials reported in the literature (Luo & Stevens, 1999; Tredici et al., 2016). A reduced yttrium (~3 mol % yttria) content is generally associated with better mechanical properties. In samples with higher yttria dopant contents, the hardness values are lower, whereas, the transparency is notably increased. The 3YSZ sample (tetragonal structure) showed the best mechanical hardness and 6YSZ and 8YSZ showed slightly lower hardness, due to higher yttria dopant content which results in the presence of a mixed tetragonal-cubic structure (6YSZ) and cubic structure (8YSZ). The changes in the averaged hardness values after the treatments for the 3YSZ and 8YSZ were not significant (paired two-tailed *t* test) while a slight increase (<2%) was found for the hardness of 6YSZ after ageing treatment. Increased hardness due to ageing was an unexpected

result, and may be due to measurement error of the hardness of pristine 6YSZ, which was notably lower than the hardness of the other pristine sample compositions.

## 5 | CONCLUSION

The combination of YSZ nanopowder and CAPAD offers a procedure for the preparation of high-density, transparent implant material suitable for the production of WttB cranial prosthesis. All the samples with yttria dopant levels ranging between 3 and 8 mol %, showed a strong resistance to LTD due to nanostructuring, as demonstrated by extended ageing simulations performed following the ISO 13356:2008. The samples were able to sustain tens of hours of treatments at 134°C; conditions equivalent to many decades of ageing in vivo. A higher yttria dopant level (8YSZ) showed higher transmittance but presented slightly lower hardness. Finally, comparison of % monoclinic transformation, optical transparency, and mechanical properties of nc-YSZ samples at baseline and following up to 100 hr hydrothermal treatments shows our implant can withstand the extended ageing treatment.

### ACKNOWLEDGMENTS

This work was supported by NSF awards #1545852 and #1547014 to GA and JEG and "Beca Mixta" from National Council of Science and Technology of Mexico (CONACYT) (741249).

### ORCID

*Nami Davoodzadeh* https://orcid.org/0000-0002-8036-5549

### REFERENCES

Aguilar, G., Davoodzadeh, N., Halaney, D., Uahengo, G., & Garay, J. E. (2018). *Influence of Low Temperature Ageing on Optical and Mechanical Properties of Transparent Yittria Stabilized-Zirconia Cranial Prosthesis*. Design and Quality for Biomedical Technologies XI, San Francisco, California: United States.

Alaniz, J. E., Perez-Gutierrez, F. G., Aguilar, G., & Garay, J. E. (2009). Optical properties of transparent nanocrystalline yttria stabilized zirconia. *Optical Materials*, *32*, 62–68.

Aminfar, A., Davoodzadeh, N., Aguilar, G., & Princevac, M. (2019). Application of optical flow algorithms to laser speckle imaging. *Microvascular Research*, *122*, 52–59.

Anselmi-Tamburini, U., Woolman, J. N., & Munir, Z. A. (2007). Transparent nanometric cubic and tetragonal zirconia obtained by high-pressure pulsed electric current sintering. *Advanced Functional Materials*, *17*, 3267–3273.

ASTM B962-13. For Testing AS, on Metal Powders MCB, Products MP. Standard Test Methods for Density of Compacted or Sintered Powder Metallurgy (PM) Products Using Archimedes' Principle. ASTM International; 2009.

Cano-Velázquez, M. S., Davoodzadeh, N., Halaney, D., Jonak, C., Binder, D., Aguilar, G., & Hernández-Cordero, J. A. (2018). Evaluation of Optical Access to the Brain in the Near Infrared Range with a Transparent Cranial Implant. Latin America Optics and Photonics Conference. Optical Society of America, Tu5C.2, Lima: Peru.

Casolco, S. R., Xu, J., & Garay, J. E. (2008). Transparent/translucent polycrystalline nanostructured yttria stabilized zirconia with varying colors. *Scripta Materialia*, *58*, 516–519.

Chevalier, J. (2006). What future for zirconia as a biomaterial? *Biomaterials*, *27*, 535–543.

Chevalier, J., Cales, B., & Drouin, J. M. (1999). Low-temperature aging of Y-TZP ceramics. *J Am Ceram Soc*, *82*, 2150–2154.

Chevalier, J., Gremillard, L., & Deville, S. (2007). Low-temperature degradation of zirconia and implications for biomedical implants. *Annual Review of Materials Research*, *37*, 1–32.

Damestani, Y., Galan-Hoffman, D. E., Ortiz, D., Cabrales, P., & Aguilar, G. (2016). Inflammatory response to implantation of transparent nanocrystalline yttria-stabilized zirconia using a dorsal window chamber model. *Nanomedicine*, *12*, 1757–1763.

Damestani, Y., Reynolds, C. L., Szu, J., Hsu, M. S., Kodera, Y., Binder, D. K., … Aguilar, G. (2013). Transparent nanocrystalline yttria-stabilized-zirconia calvarium prosthesis. *Nanomedicine*, *9*, 1135–1138.

Davoodzadeh, N. (2017). *Low-Temperature Ageing of Transparent Nanocrystalline Yttria-Stabilized-Zirconia Calvarium Prothesis*. Presented at Lasers in Surgery and Medicine, Hoboken, NJ, 440–440.

Davoodzadeh, N., Cano-Velázquez, M. S., Halaney, D. L., Jonak, C. R., Binder, D. K., & Aguilar, G. (2018). Evaluation of a transparent cranial implant as a permanent window for cerebral blood flow imaging. *Biomedical Optics Express*, *9*, 4879–4892.

Davoodzadeh, N., Cano-Velázquez, M. S., Halaney, D. L., Jonak, C. R., Binder, D. K., & Aguilar, G. (2019). *Evaluation of a Transparent Cranial Implant for Multi-Wavelength Intrinsic Optical Signal Imaging*. Neural Imaging and Sensing 2019. International Society for Optics and Photonics, 108650B.

Davoodzadeh, N., Cuando, N., Aminfar, A. H., Cano, M., & Aguilar, G. (2018, March). *Assessment of Bacteria Growth Under Transparent Nanocrystalline Yttria Stabilized-Zirconia Cranial Implant Using Laser Speckle Imaging* (Vol. 50, pp. S5–S6). Presented at Lasers in Surgery and Medicine, Hoboken, NJ.

Deville, S., Chevalier, J., & Gremillard, L. (2006). Influence of surface finish and residual stresses on the ageing sensitivity of biomedical grade zirconia. *Biomaterials*, *27*, 2186–2192.

Garay, J. E. (2010). Current-activated, pressure-assisted densification of materials [internet]. *Annual Review of Materials Research*, *40*, 445–468.

Grasso, S., Kim, B.-N., Hu, C., Maizza, G., & Sakka, Y. (2010). Highly transparent pure alumina fabricated by high-pressure spark plasma sintering. *Journal of the American Ceramic Society*, *93*, 2460–2462.

Gutierrez, M. I., Penilla, E. H., Leija, L., Vera, A., Garay, J. E., & Aguilar, G. (2017). Novel cranial implants of Yttria-stabilized zirconia as acoustic windows for ultrasonic brain therapy. *Advanced Healthcare Materials*, *6*, 1700214.

Halaney, D. L., Jonak, C., Davoodzadeh, N., Liu, J., Shah, J., Ehtiyatkar, P., … Aguilar, G. (2018). *Optical Coherence Tomography and Laser Speckle Imaging of the Brain Through a Transparent Cranial Implant in a Chronic Mouse Model*. Presented at Lasers in Surgery and Medicine, Hoboken, NJ, S10–S10.

ISO 13356:2008. (2008). Implants for surgery -- Ceramic materials based on yttria-stabilized tetragonal zirconia (Y-TZP). Retrieved from https://www.iso.org/standard/40166.html.

Keefer, K. D., & Michalske, T. A. (1987). Determination of phase transformation depth profiles with synchrotron radiation. *Journal of the American Ceramic Society*, *70*, 227–231.

Kim, D.-J., Jang, J.-W., & Lee, H.-L. (1997). Effect of tetravalent dopants on Raman spectra of tetragonal zirconia. *Journal of American Ceramic Society*, *80*, 1453–1461.

Kodera, Y., Hardin, C. L., & Garay, J. E. (2013). Transmitting, emitting and controlling light: Processing of transparent ceramics using current-activated pressure-assisted densification. *Scripta Materialia*, *69*, 149–154.

Lucas, T. J., Lawson, N. C., Janowski, G. M., & Burgess, J. O. (2015). Effect of grain size on the monoclinic transformation, hardness, roughness, and modulus of aged partially stabilized zirconia. *Dental Materials*, *31*, 1487–1492.

Lughi, V., & Sergo, V. (2010). Low temperature degradation-aging-of zirconia: A critical review of the relevant aspects in dentistry. *Dental Materials*, *26*, 807–820.

Luo, J., & Stevens, R. (1999). Porosity-dependence of elastic moduli and hardness of 3Y-TZP ceramics. *Ceramics International*, *25*, 281–286.

Muñoz-Saldaña, J., & Balmori-Ramírez, H. (2003). Mechanical properties and low-temperature aging of tetragonal zirconia polycrystals processed by hot isostatic pressing. *Journal of Materials Research*, *18*, 2415–2426.

Nakamura, K., Kanno, T., Milleding, P., & Ortengren, U. (2010). Zirconia as a dental implant abutment material: A systematic review. *The International Journal of Prosthodontics*, *23*, 299–309.

Perrichon, A., Reynard, B., Gremillard, L., Chevalier, J., Farizon, F., & Geringer, J. (2017). A testing protocol combining shocks, hydrothermal ageing and friction, applied to zirconia toughened alumina (ZTA) hip implants. *Journal of the Mechanical Behavior of Biomedical Materials*, *65*, 600–608.

Pitzer, K. S. (1982). Self-ionization of water at high temperature and the thermodynamic properties of the ions. *Journal of Physical Chemistry*, *86*, 4704–4708.

Rosenflanz, A., Frey, M., Endres, B., Anderson, T., Richards, E., & Schardt, C. (2004). Bulk glasses and ultrahard nanoceramics based on alumina and rare-earth oxides. *Nature*, *430*, 761–764.

Sanon, C., Chevalier, J., Douillard, T., & Cattani-Lorente, M. (2015). A new testing protocol for zirconia dental implants. *Dental Materials*, *31*, 15–25.

Tredici, I. G., Sebastiani, M., Massimi, F., Bemporad, E., Resmini, A., Merlati, G., & Anselmi-Tamburini, U. (2016). Low temperature degradation resistant nanostructured yttria-stabilized zirconia for dental applications. *Ceramics International*, *42*, 8190–8197.

Wei, C., & Gremillard, L. (2018). Towards the prediction of hydrothermal ageing of 3Y-TZP bioceramics from processing parameters. *Acta Materialia*, *144*, 245–256.

Xiong, Y., Fu, Z., Pouchly, V., Maca, K., & Shen, Z. (2014). Preparation of transparent 3Y-TZP nanoceramics with no low-temperature degradation. *Journal of the American Ceramic Society*, *97*, 1402–1406.

Zhang, F., Batuk, M., Hadermann, J., Manfredi, G., Mariën, A., Vanmeensel, K., … Vleugels, J. (2016). Effect of cation dopant radius on the hydrothermal stability of tetragonal zirconia: Grain boundary segregation and oxygen vacancy annihilation. *Acta Materialia*, *106*, 48–58.

Zhang, F., Vanmeensel, K., Batuk, M., Hadermann, J., Inokoshi, M., Van Meerbeek, B., … Vleugels, J. (2015). Highly-translucent, strong and aging-resistant 3Y-TZP ceramics for dental restoration by grain boundary segregation. *Acta Biomaterialia*, *16*, 215–222.

**How to cite this article:** Davoodzadeh N, Cano-Velázquez MS, Halaney DL, et al. Characterization of ageing resistant transparent nanocrystalline yttria-stabilized zirconia implants. *J Biomed Mater Res*. 2019;1–8. https://doi.org/10.1002/jbm.b.34425